

See discussions, stats, and author profiles for this publication at: <https://www.researchgate.net/publication/12270408>

# A Capillary Electrophoretic Reactor with an Electroosmosis Control Method for Measurement of Dissociation Kinetics of Metal Complexes

ARTICLE *in* ANALYTICAL CHEMISTRY · NOVEMBER 2000

Impact Factor: 5.64 · DOI: 10.1021/ac000312k · Source: PubMed

---

CITATIONS

33

---

READS

13

3 AUTHORS, INCLUDING:



Nobuhiko Iki

Tohoku University

108 PUBLICATIONS 3,206 CITATIONS

SEE PROFILE

# A Capillary Electrophoretic Reactor with an Electroosmosis Control Method for Measurement of Dissociation Kinetics of Metal Complexes

Nobuhiko Iki,\* Hitoshi Hoshino,\* and Takao Yotsuyanagi

Department of Molecular Chemistry and Engineering, Graduate School of Engineering, Tohoku University, Aoba, Aramaki, Aoba-ku, Sendai 980-8579, Japan

The solvolytic dissociation rate constants of 1:2 complexes of  $\text{Al}^{3+}$  and  $\text{Ga}^{3+}$  with an azo dye ligand, 2,2'-dihydroxyazobenzene-5,5'-disulfonate (DHABS,  $\text{H}_2\text{L}^{2-}$ ), have been evaluated with a capillary electrophoretic reactor (CER) system. This CER system is based on the fact that metal complexes encounter an overwhelming force to dissociate when apart from the ligand by CE resolution. Treatment of a capillary with a slightly acidic buffer solution, e.g., pH 5, reduces the double-layer potential ( $\zeta$ ) of the inner silica wall. Owing to slow relaxation of the deprotonation equilibria of superficial silanol groups known as the pH hysteresis, this  $\zeta$  potential can be actually retained during the electrophoresis of the metal complexes in question with a neutral buffer at pH 7.0. This method enables one to manipulate migration times, namely, residence times in a capillary tube, from 5 to 90 min, depending on the prescribed conditioning pH, without changing any other operation conditions such as buffer composition and electric field strength. The excellent performance of the CER is exemplified by the accurate estimation of the dissociation degree of the complexes. The dissociation degree–time profiles for the complexes are quantitatively described using both internal and external standards; the very inert complex of  $[\text{Co}^{\text{III}}\text{L}_2]^{5-}$  for the peak signal standardization and methyl orange for the injection volume correction. The solvolytic dissociation rate constants of the 1:2 complexes of  $\text{Al}^{3+}$  and  $\text{Ga}^{3+}$  ions with DHABS  $[\text{AlL}_2]^{5-}$  and  $[\text{GaL}_2]^{5-}$  into the 1:1 ones have been determined as  $(4.9 \pm 1.0) \times 10^{-4}$  and  $(3.7 \pm 0.3) \times 10^{-3} \text{ s}^{-1}$  at 303 K, respectively.

In actual chemical systems where metal complexes partake, the situation is frequently observed that free ligand and metal ions are steadily separated from the vicinity of metal complexes. Such a situation is the case for high-performance liquid chromatography (HPLC) of metal complexes where they move in their isolated bands along a column far apart from those of free ligand and free metal ions. Capillary electrophoresis (CE) also provides a similar

environment for metal complexes.<sup>1,2</sup> It should be noted that once metal complexes are placed in such environment, they are exposed to the overwhelming force to dissociation caused by a steep concentration jump of the ligand; inertness of the complexes is a key factor for the successful application of these methodologies. The environment provided by HPLC and CE has been of great concern to us in terms of designing kinetically controlled selectivity, the so-called kinetic differentiation (KD) mode.<sup>1–4</sup>

The kinetically controlled detection selectivity of  $\text{Al}^{3+}$ ,  $\text{Co}^{3+}$ ,  $\text{Cr}^{3+}$ ,  $\text{Cu}^{2+}$ ,  $\text{Fe}^{3+}$ , and  $\text{VO}_2^+$  ions in CE as the complexes of 2,2'-dihydroxyazobenzene-5,5'-disulfonate (DHABS,  $\text{H}_2\text{L}^{2-}$ , Figure 1) has been demonstrated in sharp contrast to the undetectability depending upon the kinetic instability of the complexes of  $\text{Cd}^{2+}$ ,  $\text{Ni}^{2+}$ , and  $\text{Zn}^{2+}$  ions.<sup>2</sup> In the course of these studies, the idea of a capillary electrophoresis reactor (CER) was provoked by the concentration jump character of the sharp band profiles in CE. It is stressed that this reactor system runs parallel with CE separation, which is of great benefit to the rate analysis in combination with the peak identification for complicated mixtures.

To date, profuse knowledge on the kinetics and mechanisms of the reaction for metal ion complexes has been compiled with some sophisticated methods mainly suitable for the fast reactions: relaxation methods with physical perturbations and nuclear magnetic resonance (NMR) spectroscopy, particularly with high-pressure techniques.<sup>5–13</sup> On the other hand, rather conventional chemical methods still are being applied to the processes in the second to minute time scale. Such methods for the dissociation processes of metal complexes given as eq 1 rely exclusively on

- (1) Iki, N.; Hoshino, H.; Yotsuyanagi, T. *Chem. Lett.* **1993**, 701–704.
- (2) Iki, N.; Hoshino, H.; Yotsuyanagi, T. *J. Chromatogr., A* **1993**, 652, 539–546. For erratum, see: *J. Chromatogr., A* **1994**, 669, 278.
- (3) Iki, N.; Hoshino, H.; Yotsuyanagi, T. *Mikrochim. Acta* **1994**, 113, 137–152.
- (4) Literature cited in ref 3.
- (5) Eigen, M.; Wilkins, R. G. *Adv. Chem. Ser.* **1965**, No. 49, 55–80.
- (6) Eigen, M. *Pure Appl. Chem.* **1963**, 6, 97–115.
- (7) Stengle, T. R.; Langford, C. H. *Coord. Chem. Rev.* **1967**, 2, 349–370.
- (8) Fiat, D.; Connik, R. E. *J. Am. Chem. Soc.* **1968**, 90, 608–615.
- (9) Deverell, C. *Prog. NMR Spectrosc.* **1969**, 4, 235–334.
- (10) Pearson, R. G.; Anderson, M. M. *Angew. Chem., Int. Ed. Engl.* **1965**, 4, 281–287.
- (11) Eldik, R. *Angew. Chem., Int. Ed. Engl.* **1986**, 25, 673–682.
- (12) Pienaar, J. J.; Kotowski, M.; Eldik, R. *Inorg. Chem.* **1989**, 28, 373–375.
- (13) Margerum, D. W.; Cayley, G. R.; Weatherburn, D. C.; Pagenkopf, G. K. In *Coordination Chemistry*; Martell, A. E., Ed.; ACS Monograph 174; American Chemical Society: Washington, DC, 1978; Vol. 2, Chapter 1.

\* To whom correspondence should be addressed. N.I.: (e-mail) iki@orgsynth.che.tohoku.ac.jp; (fax) +81-22-217-7293. H.H.: (e-mail) hoshino@analchem.che.tohoku.ac.jp; (fax) +81-22-217-7293.

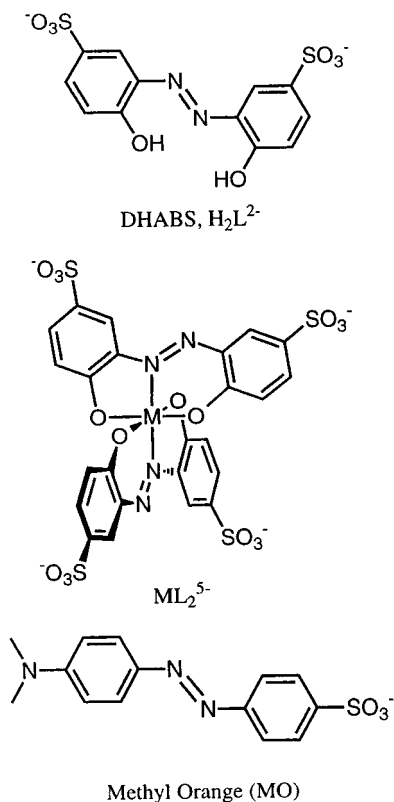
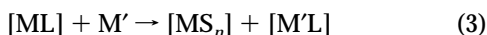
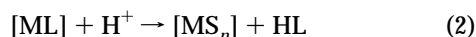
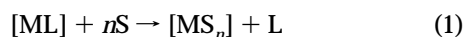


Figure 1. Structures of DHABS, the 1:2 complex with trivalent metal ion (M), and methyl orange (MO).

the substitution reactions (eqs 2–4) with proton, metal ion, and other ligands.<sup>13</sup>



where S, L', and M' denote solvent molecule, substituting ligand, and metal ion, respectively (charges of the species are omitted and the composition of the metal complexes is not necessarily 1:1). It should be noted that in fact these parallel reactions often make the elucidation of the solvolytic processes (a substitution reaction with water molecules) ambiguous. Additionally, such batch reaction systems do not seem to be reconciled with the above-mentioned circumstances experienced in HPLC and CE systems where the steep concentration jump of M and L is readily achievable in the vicinity of the complex, ML by the spatial resolution.

In this report, the direct measurements of solvolytic dissociation rates of metal complexes are described. Two attractive features of the CER are demonstrated; first a fused-silica capillary provides the reaction zone as an intact homogeneous state with no two-phase distribution event as encountered in HPLC systems, and second, the reaction time (residence time in a capillary) can be readily controlled if one can manipulate an electroosmotic flow

(EOF) rate. For this purpose, in the present work, a novel method to control EOF is developed using a "pH-hysteresis effect" of the  $\zeta$  potential at the inner wall of a capillary which actually determines the EOF. The CER system is successfully exemplified by evaluation of the dissociation rate constants of the complexes of DHABS with  $\text{Al}^{3+}$ ,  $\text{Ga}^{3+}$ , and  $\text{In}^{3+}$  ions having the stoichiometry of 1:2.

Besides HPLC and CE, the dissociation rate processes of metal complexes are of key importance in terms of the functions at work in biological systems. For example, "targeting metal complexes" for NMR diagnostic imaging and radiotherapy travel alone in the human body for rather a long lifetime before excretion.<sup>14</sup> Also, in time-resolved fluorescence schemes using Eu or Tb tags,<sup>15</sup> these metal complexes experience the environment where free metal ion and ligand are absent. The CER proposed here also can afford to serve as an experimental approach for such moderately slow decay kinetics. A comprehensive study for the estimation of association constants by CE has appeared.<sup>16</sup> The present work is the first attempt to utilize the CE system for the metal complex kinetics investigation.

## EXPERIMENTAL SECTION

**Equipment.** The capillary electrophoresis equipment with spectrophotometric detector was the same as described in the previous report.<sup>1</sup> A fused-silica capillary tube (0.05 mm i.d.) was obtained from Scientific Glass Engineering Inc. (Austin, TX). The total length,  $L$ , of a capillary was 60 cm with the effective length,  $l$ , either 15 or 45 cm (a detection window was made on the tube at 15 cm from one end). On-column detection was performed at 490 nm. The temperature of the system was kept at 303 K in a safety box with an interlock system. The spectral measurements were made with a Hitachi model U-3200 spectrophotometer. The pH was recorded with a TOA HM-5A pH meter.

**Reagents and Solutions.** Deionized (DI) water made from doubly distilled water with an Elgastat UHQ PS (Bucks, England) was used throughout the study. DHABS was synthesized with the method of Sus,<sup>17</sup> which was twice recrystallized from water, and the purity was checked by elemental analysis and  $^1\text{H}$  NMR spectroscopy.<sup>18</sup> DHABS was used as the aqueous solution ( $1.0 \times 10^{-2}$  mol  $\text{dm}^{-3}$ ). All reagents and solvents employed were of analytical grade from Kanto Chemical Co. (Tokyo, Japan). The metal ion stock solutions ( $1.0 \times 10^{-2}$  mol  $\text{dm}^{-3}$ ) were made by dissolving  $\text{AlCl}_3 \cdot 6\text{H}_2\text{O}$ ,  $\text{CoCl}_2 \cdot 6\text{H}_2\text{O}$ , and  $\text{InCl}_3 \cdot 4\text{H}_2\text{O}$  and metal Ga in diluted hydrochloric acid solution. A slightly alkaline pH buffer for complexation was 1.0 mol  $\text{dm}^{-3}$  tris(hydroxymethyl)aminomethane (Tris)-HCl buffer solution (pH 8.0). Methyl orange (MO, Figure 1) was used as an internal standard. A washing solution for the capillary consisted of 1.0 mol  $\text{dm}^{-3}$  NaOH and 1.0 mol  $\text{dm}^{-3}$  sodium dodecyl sulfate (SDS). An equimolar mixture of phosphoric acid and acetic acid solution (each 0.02 mol  $\text{dm}^{-3}$ ) was used with NaOH to prepare a conditioning buffer at a prescribed pH for the pretreatment of a fused-silica capillary. The

(14) Parker, D. *Chem. Br.* **1994**, 818–822.

(15) Diamandis, E. P. *Clin. Biochem.* **1988**, 21, 139–150.

(16) Rundlett, K. L.; Armstrong, D. W. *J. Chromatogr., A* **1996**, 721, 173–186.

(17) Sus, O. *Liebigs Ann. Chem.* **1944**, 556, 65–84.

(18) Evans, D. F.; Iki, N. *J. Chem. Soc., Dalton Trans.* **1990**, 3773–3779.

Table 1. Concentration of Total Metal and DHABS in the Injected Complex Solutions,<sup>a</sup>  $X$ ,<sup>b</sup> and Molar Absorptivities ( $\epsilon$ ) of  $[\text{ML}_2]^{5-}$

complex	$[\text{M}]_{\text{T}}/(\text{mol dm}^{-3})$	$[\text{DHABS}]_{\text{T}}/(\text{mol dm}^{-3})$	$x$	$\epsilon_{\text{M}}/(\text{cm}^{-1} \text{ dm}^3 \text{ mol}^{-1})^c$
$[\text{CoL}_2]^{5-}$	$5.0 \times 10^{-5}$	$3.0 \times 10^{-4}$	—	23 200
$[\text{AlL}_2]^{5-}$	$5.0 \times 10^{-5}$	$1.5 \times 10^{-4}$	1	32 700
$[\text{GaL}_2]^{5-}$	$1.0 \times 10^{-4}$	$3.0 \times 10^{-4}$	2	32 900
$[\text{InL}_2]^{5-}$	$2.0 \times 10^{-4}$	$6.0 \times 10^{-4}$	4	30 500

<sup>a</sup> Each solution commonly contains  $5.0 \times 10^{-5} \text{ mol dm}^{-3}$  MO and  $0.02 \text{ mol dm}^{-3}$  Tris (pH 8.0). <sup>b</sup>  $x$  is given by eq 16. <sup>c</sup> At 490 nm, estimated from the absorption spectra of the metal complexes in solution with the following composition:  $[\text{M}]_{\text{T}} = 1.0 \times 10^{-5} \text{ mol dm}^{-3}$ ,  $[\text{DHABS}]_{\text{T}} = 2.0 \times 10^{-5} \text{ mol dm}^{-3}$ ,  $[\text{Tris}]_{\text{T}} = 0.02 \text{ mol dm}^{-3}$ , and pH 8.0.

electrophoretic buffer was made with the  $0.02 \text{ mol dm}^{-3}$  phosphoric acid solution whose pH is adjusted to 7.0 with a NaOH solution.

**Sample Preparation and Injection to CE.** To a solution containing metal ion ( $\text{Al}^{3+}$ ,  $\text{Ga}^{3+}$ ,  $\text{In}^{3+}$ , or  $\text{Co}^{2+}$ ) was added the DHABS solution, the MO solution, and  $1 \text{ cm}^3$  of  $1.0 \text{ mol dm}^{-3}$  Tris-HCl buffer solution at pH 8.0. The mixture was made up to  $50 \text{ cm}^3$  and heated at  $60^\circ \text{C}$  for 15 min to complete the complex formation. The final composition of the solution is listed in Table 1 together with the molar absorptivities of the 1:2 complex at 490 nm. Divalent cobalt ion is spontaneously oxidized by dissolved dioxygen during the complexation to give  $[\text{Co(III)L}_2]^{5-}$ , which was used as an external standard. After cooling, the solution was injected from the positive end of the capillary by hydrodynamic action (height difference,  $\Delta h = 5 \text{ cm}$  for 20 s). The sample amount loaded was  $3.2 \times 10^{-9} \text{ dm}^3$ , determined with a continuous injection method.<sup>19</sup>

**Procedure for Kinetic Measurements.** A capillary is initialized by flushing with the washing solution for 10 min by suction with an aspirator, followed by rinsing thoroughly with DI water. The filling solution is replaced with the electrophoretic buffer using a gastight syringe and the sample solution containing  $[\text{Co(III)L}_2]^{5-}$  and MO is introduced as described above. The electrophoresis is initiated on applying a high voltage of 16.1–16.4 kV in a constant-current mode at  $i = 20 \mu\text{A}$ . The migration times  $t_{\text{m}}$  and the peak heights for  $[\text{Co(III)L}_2]^{5-}$  and MO are recorded. The same procedure is repeated for the  $[\text{ML}_2]^{5-}$  complexes ( $\text{M} = \text{Al, Ga, or In}$ ). To shorten the migration time  $t_{\text{m}}$ , the sample injection was followed for 20 s by additional hydrodynamic delivery of the sample band, being sandwiched with the buffer toward the negative direction ( $\Delta h = 5 \text{ cm}$  for 10 or 20 min). The electrophoresis is then started for the band located at a appropriate position in the capillary. For the longer  $t_{\text{m}}$ , the capillary is flushed by vacuum suction with the conditioning buffer ( $\text{pH}_{\text{cond}} = 4.93\text{--}5.08$ ) for 5 min, followed by switching to the pH 7.0 buffer. The sample is injected and electrophoresed as similar to that mentioned above. It is noted that on switching the polarity of the power supply output (an injection is made from the positive end) the different effective lengths  $l$  of either 15 or 45 cm are available, which is beneficial to expand the migration time window. For a total migration time less than 30 min, the shorter effective length

of  $l = 15 \text{ cm}$  is preferable; alternatively, 45 cm in  $l$  is necessary for CE experiments taking 20–90 min.

## RESULTS AND DISCUSSION

**Qualitative Description of Metal Complex Dissociation Processes in CE Systems.** A simple complexation reaction is described as,



$$K_{\text{f}} = [\text{ML}]/[\text{M}][\text{L}] \quad (5')$$

where  $K_{\text{f}}$  is the equilibrium constant. Under the conditions produced in HPLC, where M, L, and ML are separated steadily from each other, free ligand and free metal ion move away from the metal complex band. The complex is forced to dissociate unless it is inert, i.e., kinetically stable. In this practice, however, less attention seems to have been paid to the kinetic aspects of the metal complex systems at work in such a situation where the driving force for dissociation prevails. CE separates analytes by utilizing the difference in their electrophoretic mobilities in a capillary, typically in the minute time scale. The separation efficiency of CE in general is far higher in terms of the theoretical plates per meter of  $10^5\text{--}10^7$  than that of HPLC. Charged ligand and the metal complexes have different mobilities, thus allowing for a clear-cut resolution. By analogy with the HPLC system, this CE resolution, removal of ligand from the complex zone, shifts the equilibrium position entirely to the dissociation side (the left-hand side of eq 5) and thus gives rise to the inevitable splitting-off of ligand from the metal complexes, which is the solvolysis process according to reaction kinetics terminology. Conventionally, the dissociation kinetics in solutions has been traced by on mixing with acid, a substituting ligand, or metal ion as shown in eqs 2–4. In this connection, it should be stressed that the CE system provides an ideal medium for the solvolysis processes with no such “external” perturbations because the process is initiated on applying the high voltage and proceeds in a capillary all the while moving to the detection window.

**CE as a Chemical Reactor.** The basic idea of CER is to measure the decrement of peak height of the metal complex with increasing migration time in order to obtain the first-order decay curve of dissociation. Unlike HPLC, CE is by no means a two-phase system where mass transfer between phases takes place.<sup>20</sup> In addition, it has been reported that residual silanol groups on the chemically bonded silica stationary phase enhance the dissociation of metal complexes.<sup>21</sup> The plug flow profile of electroosmosis in CE is quite attractive;<sup>22</sup> unlike pressure-driven flow (Poiseuille flow) having the parabolic flow profile, the sample zone delivery by electroosmosis which minimizes the peak broadening is beneficial for the signal treatments.

Since CE can only produce one signal per one injection, using time elapsed until complex species arrive at the detection window, i.e., migration time  $t_{\text{m}}$ , it is necessary to repeat the runs with the varying  $t_{\text{m}}$  in order to obtain a signal–time relationship. The ion migrates to the detector along the distance  $l$ , under a certain

(19) Hoyt, A. M., Jr.; Sepaniak, M. J. *Anal. Lett.* **1989**, *22*, 861–873.

(20) Jeng, C.-Y.; Langer, S. H. *J. Chromatogr.* **1992**, *589*, 1–30.

(21) Uehara, N.; Kurahashi, T.; Shijo, Y. *Anal. Sci.* **1994**, *10*, 31–34.

(22) Stevens, T. S.; Cortes, H. J. *Anal. Chem.* **1983**, *55*, 1365–1375.



electric field,  $E$ ;  $t_m$  is given by eq 6,

$$t_m = l/[(\mu_{eo} + \mu_{ep})E] \quad (6)$$

where  $\mu_{eo}$  and  $\mu_{ep}$  are the mobilities caused by electroosmosis and electrophoresis, respectively.

Although four parameters in eq 6 seem to be available for the manipulation of  $t_m$ , the mobility  $\mu_{ep}$  and  $E$  are in fact not changeable for the benefit of the constancy of the reaction conditions in terms of the buffer solution environments and Joule heating. In addition, frequent changing of  $l$  for each kinetic run by switching capillary tubes to different lengths is quite impractical and is ruled out for  $t_m$  control.

From the above discussion, EOF control is of key importance to realize a CER system. Theoretically,  $\mu_{eo}$  is described as<sup>23</sup>

$$\mu_{eo} = \epsilon\zeta/\eta \quad (7)$$

where  $\epsilon$  and  $\eta$  are the permittivity and viscosity of the solution, respectively, and  $\zeta$  is the zeta potential of the inner surface of a fused-silica capillary. Only  $\zeta$  is the parameter that can be manipulated since  $\epsilon$  and  $\eta$ , the inherent physical properties of a buffer solution used, are naturally fixed. The  $\zeta$  values seems to be readily controlled by changing buffer pH or by adding modifiers in the electrophoretic buffer solution;<sup>24,25</sup> however, these approaches bring additional parameters to our CER system designing. Also, permanently coated capillaries are unusable for manipulating the  $t_m$  values because no EOF is actually expected.

The clue has been found in the pH hysteresis effect on the EOF; longer equilibration time is necessary when a particular pH is approached from the acidic pH side.<sup>26,27</sup> This phenomenon is caused by the slow response of the superficial gel layer formation and ion adsorption or ion exchange in the electric double layer to a bulk buffer pH jump.<sup>27</sup> In principle, if a capillary is pretreated with an acidic buffer at certain pH, the capillary keeps the  $\zeta$  value for a long enough time even after the running buffer of desired pH is introduced. The slower EOF can be achieved even if the reaction pH of the electrophoretic buffer is set at neutral to slightly alkaline. The EOF is to the negative end of a capillary and the sign of  $\mu_{eo}$  is positive by convention. Since the electrophoresis of the anionic metal complex  $[ML_2]^{5-}$  of DHABS takes place in the direction opposite to the EOF, the  $\mu_{ep}$  value is negative,  $-8.0 \times 10^{-4} \text{ cm}^2 \text{ V}^{-1} \text{ s}^{-1}$ .<sup>2</sup> Assuming that  $E = 300 \text{ V cm}^{-1}$  and  $l = 15 \text{ cm}$ , we can roughly estimate the  $t_m$  value of the  $[ML_2]^{5-}$  from 3 to 30 min by changing the  $\mu_{eo}$  from  $8.3 \times 10^{-4}$  to  $11 \times 10^{-4} \text{ cm}^2 \text{ V}^{-1} \text{ s}^{-1}$ , as calculated by eq 6. Under similar conditions with longer  $l$ , 45 cm, the  $t_m$  is changed from 9 to 90 min. These wide reaction time windows seem to be sufficient to cover the dissociation degrees of metal complexes necessary for accurate rate analyses. Thus, the CER owes its success to this new EOF controlling method.

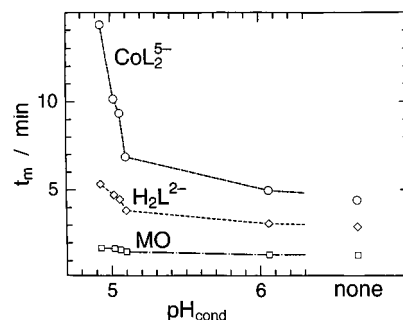


Figure 2. Effect of conditioning pH for fused-silica capillary on the migration time of species. Conditioning buffer:  $[H_3PO_4]_T = [CH_3COOH]_T = 0.02 \text{ mol dm}^{-3}$ ,  $pH_{\text{cond}} = 4.93\text{--}6.10$  with NaOH. Electrophoretic buffer:  $[H_3PO_4]_T = 0.02 \text{ mol dm}^{-3}$ , pH 7.0 with NaOH. Electrophoresis at  $T = 303 \text{ K}$ ,  $i = 20 \mu\text{A}$ ,  $V = 16.2\text{--}16.4 \text{ kV}$ ,  $l = 15 \text{ cm}$ , and  $L = 60 \text{ cm}$ .

Figure 2 shows the  $t_m$  of the species at various conditioning pHs for the fused-silica capillary surface in comparison with those obtained with an unconditioned capillary. It should be noted that all the  $t_m$  were measured at the same pH 7 after conditioning on acidic side of pH 4.9–6.1. The  $t_m$  values of  $[Co^{III}L_2]^{5-}$  decrease steeply around pH 5 where the EOF, that is, the  $\zeta$  potential, is known to be sensitive over this pH range.<sup>25–27</sup> When  $\mu_{eo}$  is calculated with the  $t_m$  values of the solvent peak, it varies only from  $9.15 \times 10^{-4}$  to  $10.83 \times 10^{-4} \text{ cm}^2 \text{ V}^{-1} \text{ s}^{-1}$  in this pH range. This small increment in  $\mu_{eo}$  induces a great change of  $t_m$  for the highly charged complex  $[Co^{III}L_2]^{5-}$  as predicted by eq 6. Additionally, no significant change in the  $t_m$  for repeated injections of  $[Co^{III}L_2]^{5-}$  was observed because of the very slow relaxation of the  $\zeta$  potential once established in acidic solutions.<sup>26,27</sup> This method does not require special reagents, modifiers, and coating of capillary which possibly give serious perturbation to the dissociation kinetics.<sup>25,26</sup> Regeneration of the capillary is easily made by washing with NaOH solution containing SDS (see the procedure in the Experimental Section).

Table 2 summarizes the obtained  $t_m$  at various conditioning pHs and  $l$  as well as the residual ratios for  $[ML_2]^{5-}$ . For the shorter reaction time, a  $t_m$  value as small as 1.2 min was obtained by squeezing the sample zone to a prescribed position with a siphonaction prior to the electrophoresis. As shown in Table 2, when the polarity is inverted 3 times longer  $t_m$  was also obtained ( $l$ , from 15 to 45 cm). There seems to have been no report on utilization of slow acid dissociation equilibria of the capillary surface to control EOF. Control of EOF is sometimes crucial to separate solutes possessing  $e\mu_{ep}$  values very close to each other.<sup>28</sup> In such circumstances, this new EOF control method is quite applicable for resolution enhancement.

**Derivation of the Rate Constants of Dissociation of  $[ML_2]^{5-}$  in CER.** Accurate measurements of the dissociation processes of  $[ML_2]^{5-}$  are realized using the double standardization technique. MO is added as an internal standard for correcting for the injection volume, while an external standard,  $[Co^{III}L_2]^{5-}$ , is for estimation of the concentration of remaining  $[ML_2]^{5-}$  that survived during migration in the capillary. For the CE run for the solution containing  $[Co^{III}L_2]^{5-}$  and MO (for example, see Figure

(23) Rice, C. J.; Whitehead, R. J. *J. Phys. Chem.* **1965**, *69*, 4017–4024.

(24) Li, S. F. Y. *Capillary Electrophoresis*; Journal of Chromatography Library 52; Elsevier: Amsterdam, 1992; Chapters 4 and 5.

(25) Schomburg, G.; Belder, D.; Gilges, M.; Motsch, S. *J. Capillary Electrophor.* **1994**, *1*, 219–230.

(26) Lambert, W. J.; Middleton, D. L. *Anal. Chem.* **1990**, *62*, 1585–1587.

(27) Schwer, C.; Kenndler, E. *Anal. Chem.* **1991**, *63*, 1801–1807.

(28) Terabe, S.; Yashima, T.; Tanaka, N.; Araki, M. *Anal. Chem.* **1988**, *60*, 1673–1677.

Table 2. Summary of Parameters Determined and Residual Ratios for  $[\text{ML}_2]^{5-}$  Complexes

$\text{pH}_{\text{cond}}^a$	$l/\text{cm}$	metal	$t_m/\text{min}$	$H_{\text{MO}}/\text{cm}$	$H_{\text{ML}_2}/\text{cm}$	$R_M/R_{\text{Co}}$	$[\text{ML}_2^{5-}]/[\text{ML}_2^{5-}]_0$
none	15	Co	4.4	10.12	12.62	1	1
		Al	4.3	10.44	18.22	1.40	0.99 <sup>c</sup>
		Ga	4.7	11.38	12.30	0.86	0.36
$t_p/\text{min}^b$	10	Co	2.8	5.7	8.3	1	1
		Ga	2.8	3.4	7.2	1.45	0.51
20	15	Co	1.2	3.0	5.8	1	1
		Ga	1.2	3.3	12.5	1.93	0.68
		Ga	1.2	4.2	16.2	1.98	0.70
5.10	15	Co	6.9	7.09	7.13	1	1
		Al	6.8	6.14	8.00	1.30	0.92
		Ga	6.6	6.48	3.85	0.59	0.21
	45	Co	19.1	5.10	4.98	1	1
		Al	18.6	5.03	4.41	0.90	0.64
		Ga	18.0	4.94	0.40	0.08	0.03 <sup>c</sup>
5.06	15	Co	9.4	5.43	5.60	1	1
		Al	9.2	4.62	4.48	0.94	0.67
		Ga	8.6	4.90	1.22	0.41	0.15
	45	Ga	8.4	4.79	1.37	0.47	0.17
		Co	25.2	5.45	4.71	1	1
		Al	24.5	5.24	3.25	0.72	0.51
5.02	15	Co	10.2	5.86	5.29	1	1
		Al	10.5	8.98	8.52	1.05	0.75
		Co	30.2	3.83	2.84	1	1
	45	Al	28.5	3.38	1.48	0.59	0.42
		Co	14.3	4.00	2.70	1	1
		Ga	13.4	3.31	0.35	0.16	0.05

<sup>a</sup>  $\text{pH}_{\text{cond}}$ , conditioning pH for EOF control. <sup>b</sup>  $t_p$ , time for driving the injected sample zone toward a detector side by siphonic action ( $\Delta h = 5$  cm).  
<sup>c</sup> Omitted in the plots in Figure 7.

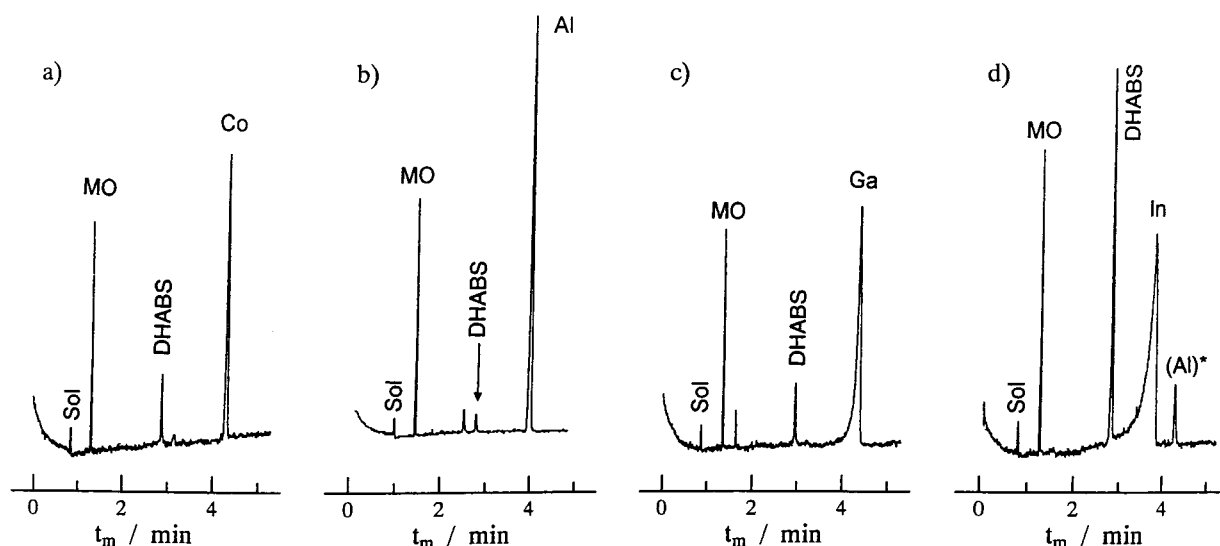


Figure 3. Typical electropherograms for the  $[\text{ML}_2]^{5-}$  systems: (a)  $\text{Co}^{\text{III}}$ , (b)  $\text{Al}$ , (c)  $\text{Ga}$ , and (d)  $\text{In}$ . Composition is listed in Table 1. Sol, solvent peak; MO, methyl orange; DHABS, free DHABS; In,  $[\text{InL}]^-$  complex and the product species and  $\text{Al}^*$ ,  $[\text{AlL}_2]^{5-}$  from contaminant, respectively, in electropherogram. Other conditions are the same as shown in Figure 2.

3a), each peak height  $H$  is given as

$$H_{\text{MO},1} = \kappa_{\text{MO}} \epsilon_{\text{MO}} [\text{MO}] \nu_{\text{inj},1} \quad (8)$$

$$H_{\text{Co},1} = \kappa_{\text{Co}} \epsilon_{\text{Co}} [\text{CoL}_2^{5-}] \nu_{\text{inj},1} \quad (9)$$

where  $\kappa_{\text{MO}}$  and  $\kappa_{\text{Co}}$  are proportional constants,  $\epsilon_{\text{MO}}$  and  $\epsilon_{\text{Co}}$  are the molar absorptivities for MO and  $[\text{CoL}_2]^{5-}$ , and  $\nu_{\text{inj}}$  is injection volume (see the Appendix for the definition of  $\kappa$ ). In general, a

$\text{Co}^{3+}$  ion having low-spin  $d^6$  electron configuration forms kinetically inert complexes.<sup>29</sup> Actually, even in the presence of  $10^{-4}$  mol  $\text{dm}^{-3}$  EDTA, no evidence was seen for the replacement of the  $[\text{Co}^{\text{III}}\text{L}_2]^{5-}$  complex with EDTA at pH 8.0 within 1 h.<sup>30</sup> The  $[\text{Co}^{\text{III}}\text{L}_2]^{5-}$  complex is suitable as an external standard because it has a  $\mu_{\text{ep}}$  value close to those of the DHABS complexes of trivalent metal ions studied here such as  $\text{Al}(\text{III})$ ,  $\text{Ga}(\text{III})$ , and  $\text{In}(\text{III})$ .

(29) Basolo, F.; Pearson, R. G. *Mechanisms of Inorganic Reactions*, 2nd ed.; John Wiley and Sons: New York, 1967; Chapter 3.

(30) Iki, N. Unpublished results, 1993.

For the kinetic analysis of  $[\text{ML}_2]^{5-}$ , the peak height signals were exclusively employed because the peak area data may give erratic results which are caused by the asymmetric peak profiles due to dissociation products such as the 1:1 complex of  $[\text{ML}]^-$  and free DHABS (see below for  $[\text{GaL}_2]^{5-}$  and  $[\text{InL}_2]^{5-}$  systems). For the run of  $[\text{ML}_2]^{5-}$  under conditions similar to  $[\text{Co}^{\text{III}}\text{L}_2]^{5-}$ ,  $H$  are similarly given by eqs 10 and 11.

$$H_{\text{MO},2} = \kappa_{\text{MO}}\epsilon_{\text{MO}}[\text{MO}]\nu_{\text{inj},2} \quad (10)$$

$$H_{\text{M},2} = \kappa_{\text{M}}\epsilon_{\text{M}}[\text{ML}_2^{5-}]\nu_{\text{inj},2} \quad (11)$$

The peak height signals of  $[\text{Co}^{\text{III}}\text{L}_2]^{5-}$  and  $[\text{ML}_2]^{5-}$  are normalized by that of MO in each run,

$$R_{\text{Co}} = H_{\text{Co},1}/H_{\text{MO},1} \quad (12)$$

$$R_{\text{M}} = H_{\text{M},2}/H_{\text{MO},2} \quad (13)$$

In addition, the  $R_{\text{M}}$  is corrected with that of the Co complex, thus we obtain,

$$R_{\text{M}}/R_{\text{Co}} = \kappa_{\text{M}}\epsilon_{\text{M}}[\text{ML}_2^{5-}]/\kappa_{\text{Co}}\epsilon_{\text{Co}}[\text{CoL}_2^{5-}] \quad (14)$$

As mentioned earlier, since the trivalent metal complexes of  $[\text{Co}^{\text{III}}\text{L}_2]^{5-}$  and  $[\text{ML}_2]^{5-}$  behave very similarly in terms of size and charge, the assumption of  $\kappa_{\text{Co}} = \kappa_{\text{M}}$  is acceptable (the validation of this assumption is given in the Appendix). Then eq 14 is rewritten as,

$$R_{\text{M}}/R_{\text{Co}} = \epsilon_{\text{M}}[\text{ML}_2^{5-}]/\epsilon_{\text{Co}}[\text{CoL}_2^{5-}] \quad (15)$$

When the ratio of the initial concentrations (subscript 0) of  $[\text{ML}_2]^{5-}$  and  $[\text{Co}^{\text{III}}\text{L}_2]^{5-}$  is taken as  $x$ , we obtain,

$$[\text{ML}_2^{5-}]_0 = x[\text{CoL}_2^{5-}]_0 \quad (16)$$

Also, assuming that the  $[\text{Co}^{\text{III}}\text{L}_2]^{5-}$  is sufficiently stable during electrophoresis,

$$[\text{CoL}_2^{5-}] = [\text{CoL}_2^{5-}]_0 \quad (17)$$

therefore,

$$[\text{ML}_2^{5-}]_0 = x[\text{CoL}_2^{5-}] \quad (18)$$

Introducing eq 18 into eq 15, a ratio of the concentration of  $[\text{ML}_2]^{5-}$  at the detection point against the initial concentration (a residual ratio) is given by eq 19. All the parameters in the right-

$$[\text{ML}_2^{5-}]/[\text{ML}_2^{5-}]_0 = \epsilon_{\text{Co}}R_{\text{M}}/x\epsilon_{\text{M}}R_{\text{Co}} \quad (19)$$

hand side of eq 19 can be measured or known. Because solvolytic dissociation reaction follows the first-order kinetics, the rate law

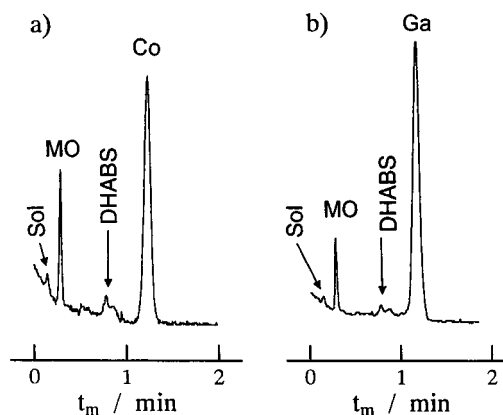


Figure 4. Typical electropherograms for (a)  $[\text{Co}^{\text{III}}\text{L}_2]^{5-}$  and (b)  $[\text{GaL}_2]^{5-}$  complexes at shorter  $t_{\text{m}}$ . The sample zone was driven toward a negative end for 20 min by hydrodynamic action. No conditioning buffer was used in this experiment. Other conditions are the same as shown in Figure 2.

is given by,

$$d[\text{ML}_2^{5-}]/dt = k_{\text{d}}[\text{ML}_2^{5-}] \quad (20)$$

Integrating eq 20 from  $t = 0$  to  $t_{\text{m}}$  yields eq 21.

$$\ln([\text{ML}_2^{5-}]/[\text{ML}_2^{5-}]_0) = -k_{\text{d}}t_{\text{m}} \quad (21)$$

Here we can obtain  $k_{\text{d}}$  by fitting eq 21 using the data obtained with eq 19 at various  $t_{\text{m}}$ .

**Reaction Rates.** DHABS is one of the 2,2'-dihydroxyazo family commonly seen in spectrophotometry for metal ions.<sup>31</sup> Particularly, DHABS forms stable 1:2 complexes  $[\text{ML}_2]^{5-}$  with trivalent metal ions via  $\text{O}^-$ ,  $\text{N}$ , and  $\text{O}^-$  coordination (Figure 1) under acidic to slightly alkaline conditions.<sup>2,18</sup> Table 1 lists the molar absorptivities at 490 nm of the DHABS complexes. Since the acid dissociation constants of two OH groups have been determined as  $\text{p}K_{\text{a}1} = 6.8$  and  $\text{p}K_{\text{a}2} = 9.9$  at 298 K,  $I = 0.1$  M by spectrophotometric titrations, the predominant species of DHABS in the electrophoretic buffer at pH 7 are  $\text{H}_2\text{L}^{2-}$  and  $\text{HL}^{3-}$ .<sup>30</sup>

Typical electropherograms for each complex are shown in Figure 3. As can be seen, the  $t_{\text{m}}$  values of  $[\text{Co}^{\text{III}}\text{L}_2]^{5-}$ ,  $[\text{AlL}_2]^{5-}$ , and  $[\text{GaL}_2]^{5-}$  are almost identical. In the case of the Ga system, the leading peak pattern of  $[\text{GaL}_2]^{5-}$  suggests the partial dissociation of the  $[\text{GaL}_2]^{5-}$  complex; the products of the reaction,  $[\text{GaL}]^-$ ,  $\text{H}_2\text{L}^{2-}$ , and  $\text{HL}^{3-}$ , move faster on the EOF (smaller  $|\mu_{\text{ep}}|$ ) than the  $[\text{GaL}_2]^{5-}$  ion does. Even at  $t_{\text{m}} = 4$  min, the residual ratio of  $[\text{GaL}_2]^{5-}$  is calculated to be only 36% (Table 2), which is about  $1/e$  to the initial concentration. To reduce the dissociation degree of  $[\text{GaL}_2]^{5-}$  the reaction time, i.e.,  $t_{\text{m}}$ , should be shortened, driving the sample zone toward the negative side by siphon action before the electrophoresis at the sacrifice of peak sharpness. As shown in Figure 4, the peaks for MO,  $[\text{Co}^{\text{III}}\text{L}_2]^{5-}$ , and  $[\text{GaL}_2]^{5-}$  are a little broadened; in fact, the peak leading is rather reduced. For the extreme case for the  $[\text{InL}_2]^{5-}$  complex whose dissociation is too fast on the CE time scale, no peaks were found for this complex

(31) Ueno, K.; Imamura, T.; Cheng, K. L. *Handbook of Organic Analytical Reagents*; CRC Press Inc.: Boca Raton, FL, 1982; pp 145–157.

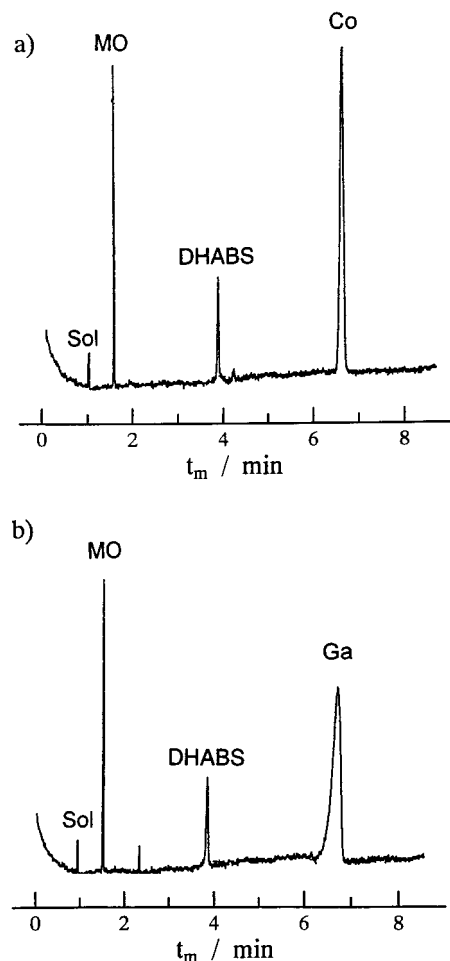


Figure 5. Typical electropherograms for (a)  $[\text{Co}^{\text{III}}\text{L}_2]^{5-}$  and (b)  $[\text{GaL}_2]^{5-}$  complexes at longer  $t_m$ .  $\text{pH}_{\text{cond}} 5.10$ . Other conditions are the same as shown in Figure 2.

species even at the small  $t_m$  values from 1.2 to 2.8 min. It should be noted that in the  $[\text{InL}_2]^{5-}$  system the first large peak at 3.6 min is due to the fast-moving products, probably  $[\text{InL}]^-$ ,  $\text{H}_2\text{L}^{2-}$ , and  $\text{HL}^{3-}$ , and the second one at 4.3 min is of the  $[\text{AlL}_2]^{5-}$  species as a contaminant in the  $\text{In}^{3+}$  solution.

The new EOF control method was very successful for expanding the residence time window in a capillary for the Al and Ga complexes. Some examples are shown in Figures 5 and 6. The leading peak shape became more significant for  $[\text{GaL}_2]^{5-}$  at a longer  $t_m$  of 6.64 min (Figure 5), reflecting an increase in dissociation. At  $t_m = 25$  min (Figure 6), the  $[\text{AlL}_2]^{5-}$  peak height is significantly lowered as compared with that shown in Figure 3a and b, which indicates that  $\sim 50\%$  decay of the complex was achieved.

In Figure 7, where the linear dependence of the logarithmic residual ratio values on  $t_m$  are shown, first-order decay kinetics is demonstrated for both Al and Ga. The decay rate constants,  $k_d$ , are calculated from the slopes of the plots to be  $4.9 \times 10^{-4} \text{ s}^{-1}$  for the  $[\text{AlL}_2]^{5-}$  complex and  $3.7 \times 10^{-3} \text{ s}^{-1}$  for the  $[\text{GaL}_2]^{5-}$  one at 303 K. The intercepts on the ordinate of Figure 7 are 1.024 and 0.962 for Al and Ga, respectively. These values are most likely biased from unity ( $[\text{ML}_2^{5-}]/[\text{ML}_2^{5-}]_0 = 1$ ) at  $t_m = 0$  by the relatively long extrapolation. Just after the electrophoresis is started, the zone overlapping between  $[\text{ML}_2]^{5-}$  and free DHABS

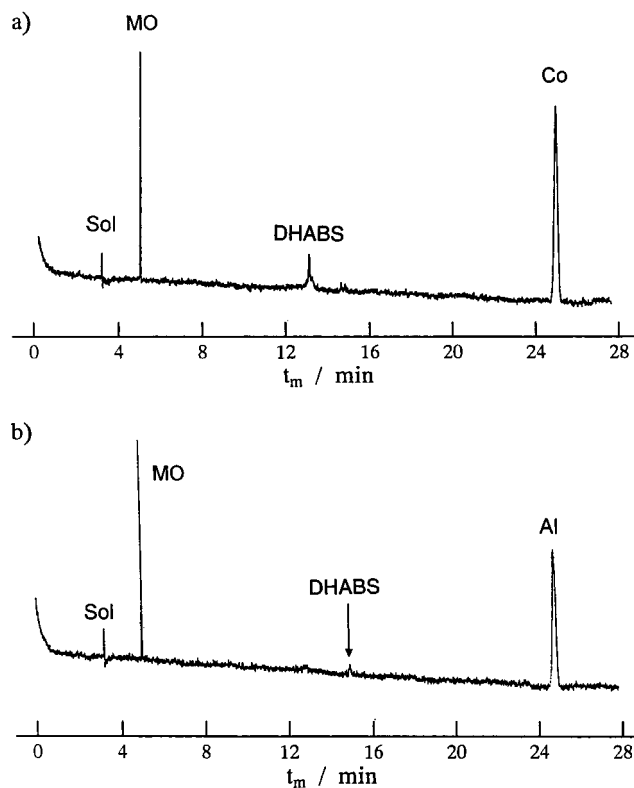


Figure 6. Typical electropherograms for (a)  $[\text{Co}^{\text{III}}\text{L}_2]^{5-}$  and (b)  $[\text{AlL}_2]^{5-}$  complexes at longer  $t_m$ .  $\text{pH}_{\text{cond}} 5.06$ ,  $l = 45$  cm, and  $L = 60$  cm. Other conditions are the same as shown in Figure 2.

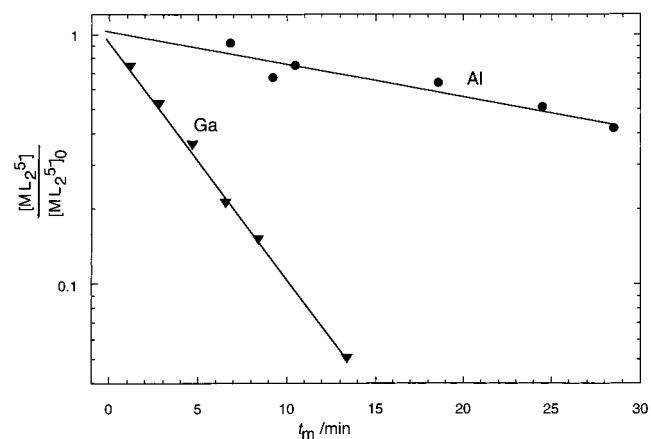


Figure 7. Reaction profiles obtained for  $[\text{AlL}_2]^{5-}$  and  $[\text{GaL}_2]^{5-}$  by CER. The raw data are given in Table 2. For conditions, see the captions in Figures 2–6.

possibly causes retardation of the complex dissociation. In fact, this likelihood is negligible because each zone length is only 1.6 mm and the zone overlapping time is calculated as merely 5.6 s for all cases. In this CER system, a decrease in the peak height absorbance of  $[\text{ML}_2]^{5-}$  is traced and its decay curve is readily obtained. The fact that the high-resolution CE separates the products as soon as they are produced is very beneficial, in particular, when the absorption spectra of the products and the reactant severely overlap. In the DHABS complex systems where the spectrally overlapping species,  $[\text{ML}_2]^{5-}$ ,  $[\text{ML}]^-$ ,  $\text{H}_2\text{L}^{2-}$ , and  $\text{HL}^{3-}$  are present, the batch reaction system is by no means practical for cross-check purposes to validate the above  $k_d$  values.



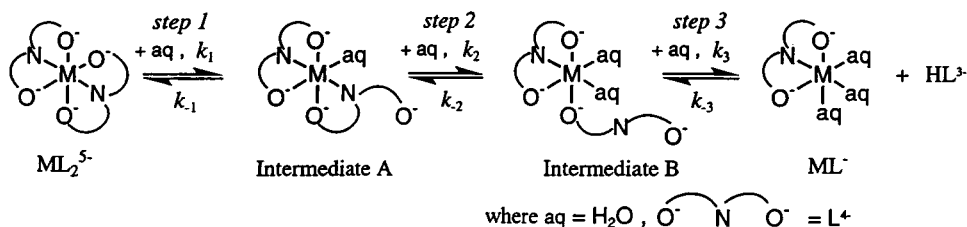


Figure 8. Possible reaction mechanism of dissociation of  $[\text{ML}_2]^{5-}$  to  $[\text{ML}]^-$ . The  $\text{HL}^{3-}$  species are involved in the fast protonation equilibria, thus giving the equilibrium mixture of  $\text{HL}^{3-}$  and  $\text{H}_2\text{L}^{2-}$  at pH 7.0.

It should be stressed that the simplicity of the CER liberates one from the complicated and tedious task of analyzing time–absorbance data obtained in the ordinary solution kinetic experiments.

**Brief Description of the Dissociation Reaction Mechanisms.** Although the interpretation of the  $k_d$  values obtained here and the detailed mechanisms of the dissociation processes of DHABS complexes are beyond the scope of this article, the course of the reactions is outlined here in relation to the highlighted features of the CER system.

The adherence of the data to the first-order rate law as shown in Figure 7 does not necessarily guarantee a simple reaction mechanism. The successive dissociation processes of  $[\text{ML}_2]^{5-}$  are most likely the case; the dissociation of  $[\text{ML}_2]^{5-}$  into  $[\text{ML}]^-$  and free DHABS is followed by the elimination of  $\text{L}^{4-}$  from  $[\text{ML}]^-$ , leaving  $\text{M}^{3+}$  ion and free DHABS. As shown in the In system (Figure 3), the peak due to  $[\text{InL}]^-$  is found at 3.6 min. In addition, the leading peak profile of the  $[\text{GaL}_2]^{5-}$  complex suggests that a similar 1:1 species having a smaller  $\mu_{\text{ep}}$  is involved in the product mixture. In the Al system, such peak leading seems to be very subtle since the  $[\text{AlL}_2]^{5-}$  species has the slowest dissociation rate. It is conceivable that the observed rate constant  $k_d$  in the Al and Ga systems corresponds to the first dissociation process. Based on a reasonable assumption that cleavage of three coordination bonds between  $\text{M}^{3+}$  ion and the ligand occurs in a certain sequence, a plausible dissociation mechanism is given in Figure 8.

The backward reactions of steps 1 and 2 may be overwhelmingly fast as compared with the forward ones of steps 2 and 3 because the coordination atoms such as  $\text{O}^-$  and N are still placed in close vicinity to the central  $\text{M}^{3+}$  ion in intermediates A and B. It is noted that step 3 is a bimolecular process and actually irreversible because the concentrations of the products,  $[\text{ML}]^-$  and DHABS, are drastically reduced in the reaction zone by the CE separation. Hence, the step 3 is most likely the rate-determining step of the dissociation of  $[\text{ML}_2]^{5-}$  to  $[\text{ML}]^-$  taking steps 1 and 2 as the preequilibria. In fact, only a slight difference was found in the  $\mu_{\text{ep}}$  values of  $[\text{AlL}_2]^{5-}$  and  $[\text{GaL}_2]^{5-}$  from that of the nondissociative complex of  $[\text{Co}^{\text{III}}\text{L}_2]^{5-}$  (the maximum differences in  $\mu_{\text{ep}}$  were 11.5% at  $t_m = 8.4$  min and 5.6% at  $t_m = 28.5$  min in the Ga and Al systems, respectively. See Table 2.). The intermediates A and B cannot be identified at least electrophoretically. These suggest that accumulation of the intermediates A and/or B is not significant during the reaction. The detailed mechanistic interpretation of these azo complexes will be described elsewhere.

Table 3 summarizes the solvolysis rate constants obtained with the CER system in comparison with those of the free aqua ions.

Table 3. Dissociation Reaction Rate Constants at 303 K and Water Exchange Rate Constants of Al(III) and Ga(III) Ions at 298 K

	$k_d/\text{s}^{-1}$		$k_{\text{ex}}/\text{s}^{-1}$ <sup>a</sup>
$[\text{AlL}_2]^{5-}$	$(4.9 \pm 1.0) \times 10^{-4}$ $[(2.95 \pm 0.60) \times 10^{-2} \text{ min}^{-1}]$	Al(III)	1.29
$[\text{GaL}_2]^{5-}$	$(3.7 \pm 0.3) \times 10^{-3}$ $[(2.21 \pm 0.24) \times 10^{-1} \text{ min}^{-1}]$	Ga(III)	$4.00 \times 10^2$

<sup>a</sup> Taken from ref 32.

The values of  $k_d$ , which are several orders of magnitude smaller than those of  $k_{\text{ex}}$ , seem to have no simple relations with the water exchange kinetics. It is noted that in general the readily available  $k_{\text{ex}}$  tabulation can hardly be used as a good measure of the complex solvolysis processes.

## CONCLUSION

In this study, it has been successfully demonstrated that CE serves as a chemical reactor for measurements of dissociation kinetics of metal complexes. No doubt the facile control of migration time using the pH hysteresis of EOF can afford to realize the CER. Also such attractive features of CE as the plug-flow profile, no interactions with a secondary phase, and the parallel scheme of dissociation and separation allow the simple treatment of data. It is emphasized that the proper  $t_m$  reference materials are available (as  $[\text{Co}^{\text{III}}\text{L}_2]^{5-}$  in our case); the CER can actually extend its applications to a great number of metal complexes. From a practical viewpoint, the CER will bring good knowledge for designing tactics of kinetically stable complexes for biological targeting use and for HPLC/HPCE methodologies, shedding light on the underlying chemistry of such metal complex functions.

## APPENDIX

**Validity of the Assumption,  $\kappa_M = \kappa_{\text{Co}}$ .** If the Gaussian peak profile approximation stands for the zone profile for  $[\text{ML}_2]^{5-}$ , the peak height is given by

$$H_M = \epsilon_M [\text{ML}_2^{5-}] \nu_{\text{inj}} / (\sqrt{2\pi} \sigma_M) \quad (\text{A-1})$$

where  $\sigma_M$  is the standard deviation of the  $[\text{ML}_2]^{5-}$  peak. By comparing with eq 11,  $\kappa_M$  is given by

$$\kappa_M = 1/(\sigma_M) \quad (\text{A-2})$$

which expresses the degree of zone broadening. It is noted that

zone broadening due to product species such as  $\text{HL}^{3-}$  or  $\text{ML}^-$  is ruled out. Theoretically  $\sigma$  is given by<sup>33</sup>

$$\sigma_{\text{M}} = \sqrt{2D t_{\text{m}}} \quad (\text{A-3})$$

where  $D$  is a diffusion coefficient of  $[\text{ML}_2]^{5-}$ .

The migration time,  $t_{\text{m}}$  is a function of  $\mu_{\text{ep}}$  (see eq 6) under given conditions; in the simplest theory,  $\mu_{\text{ep}}$  obeys Stokes' law.

$$\mu_{\text{ep}} = ez/6\pi\eta a \quad (\text{A-4})$$

where  $e$ ,  $z$ , and  $a$  are elementary electric charge, the number of total charge, and the radius of solutes, respectively.<sup>34</sup> Also, the diffusion coefficient is given as

$$D = k_{\text{B}}T/6\pi\eta a \quad (\text{A-5})$$

where  $k_{\text{B}}$  and  $T$  are the Boltzmann constant and absolute

temperature, respectively. While the distance between two sulfonate functions on DHABS is calculated as large as 0.602 nm by the MM2 method, the ionic radii in nanometers of the metal ions (6-fold coordination) are as follows:  $\text{Al}^{3+}$ , 0.068;  $\text{Ga}^{3+}$ , 0.076; and  $\text{Co}^{3+}$  (low spin), 0.069.<sup>35</sup> Therefore, there are virtually no differences in the  $a$  among the  $[\text{ML}_2]^{5-}$  ions. As a result, the CE behavior of the  $[\text{ML}_2]^{5-}$  should be very similar in terms of  $t_{\text{m}}$  and  $D$ , which indicates that  $\sigma_{\text{M}}$  in eq A-3 is practically identical among the complexes, namely,  $\kappa_{\text{M}} = \kappa_{\text{Co}}$ . This validity is experimentally given by the fact that the  $[\text{AlL}_2]^{5-}$  and  $[\text{CoL}_2]^{5-}$  complexes comigrate.<sup>2</sup>

Received for review March 15, 2000. Accepted July 12, 2000.

AC000312K

(32) Lincoln, S. F.; Merbach, A. E. *Adv. Inorg Chem.* **1995**, *42*, 1–88.

(33) Jorgenson, J. W.; Lukacs, K. D. *Anal. Chem.* **1981**, *53*, 1298–1302.

(34) Weinberger, R. *Practical Capillary Electrophoresis*. Academic Press: San Diego, CA, 1993; Chapter 2.

(35) Cotton, F. A.; Wilkinson, G.; Murillo, C. A.; Bochmann, M. *Advanced Inorganic Chemistry*, 6th ed.; Wiley-Interscience: New York, 1999; pp 1301–1304.